International Journal of Enhanced Research in Science Technology & Engineering, ISSN: 2319-7463
Vol. 3 Issue 6, June-2014, pp: (99-105), Impact Factor: 1.252, Available online at: www.erpublications.com

Design and analysis of a low cost seismic data recorder

Voutsinas S.[1], Dilintas G.[2], Voulgaris N.[3]

[1,2]Technological and Educational Institute of Piraeus, Department of Electronic computing systems, TEI of Piraeus Campus- Aigaleo - ATHENS GR 12244

[3]Department of Geophysics - Geothermics, Faculty of Geology and Geoenvironment, National and Kapodistrian University of Athens, University Campus- Zografou- Athens GR 15784

Abstract: Earthquakes represents significant natural hazard. Although they cannot be predicted, it is possible to mitigate earthquake risk. This can be achieved by using dense networks of seismic data recorders that continuously monitor seismic activity. The objective of this article is to introduce the design of a digital data recorder, capable of earthquake monitoring. The implementation proposed here is based in low cost equipment that involves Micro ElectroMechanical Systems (MEMS) sensors, custom geophone sensors, and open source tools for software development. Although this recorder is based on Commercial Off-The-Shelf (COTS) components it does not deviate from the standards set by international organisations for seismic data recorders.

Keywords: Cortex CPU, Delta - sigma ADC, Digitizer, Early Warning Systems, Ultra-low noise filtering.

Introduction

The complex nature of earthquakes currently renders the problem of precise earthquake prediction impossible to solve. Human societies though can compensate the risk of an upcoming earthquake, by the use of Earthquake Early Warning systems (EEW) [1]. Historically, J.D. Cooper introduced the idea of an earthquake early warning system in 1868. Cooper suggested the installation of seismic detectors, which when triggered would transmit a signal via the telegraph network so that the citizens of San Francisco would be alarmed. However, a whole century passed until the idea was first implemented in order to protect the railway of Tohoku Shinkansen [2].

During an earthquake several types of seismic waves are produced, such as Primary Waves (P-Waves), Secondary Waves (S-Waves) and Surface Waves. Each wave propagates with a different velocity, thus P and S waves arrive separately at a given monitoring node. The main principle of EEW systems is the continuous real-time monitoring of seismic activity and more specifically the observation of P-waves. By analyzing the P-wave arrivals, estimation of the earthquake's magnitude, epicentral distance, arrival time and peak ground motion parameters can be achieved [3]. There is a large drawback in the development of EEW systems: as the warning time increases, so does the uncertainty in the estimated shaking intensity [4].

The implementation of EEW systems is based on dense networks of data recorders. One of the most advanced EEW was developed by the National Research Institute for Earth Science and Disaster Prevention (NIED), and the Japan Meteorological Agency (JMA), consisting of 1089 nodes and with mean interstation distances 18.7 km [5].

Following the evolution of digital circuits, analog recorders began to give way to the new technology. Digital recorders are smaller in size; they do not require any consumables and provide high quality recordings. Finally they have an embedded digital signal processor, in order to process the seismic signals instantaneously.

Objective

Our objective is to design and construct a low cost recorder for seismic waveform data, based on Commercial Off - The - Shelf (COTS) components, which can in turn be combined to form an EEW network. COTS based nodes may not be as accurate as the nodes that bear electromechanical sensors, but due to their low cost, the density of the EEW network can be increased. Consequently, a network with more nodes will provide an increased amount of seismic data leading to improved accuracy and significant reduction of false alarms.

Methods and materials

To achieve the above objective, the standards set by global organizations [6] were studied, so that the recorder could be compatible with various devices and sensors. Furthermore, several sensors were examined in order to choose the appropriate ones to equip our recorder by default. Regarding the software part required for the mathematical analysis and the firmware development of the recorder, open source tools have been selected, like octave for the mathematical analysis of the system's components and Energia IDE for the development of the firmware.

Digital data recorders mainly consist of several sub-systems, which are shown in figure 1 below.

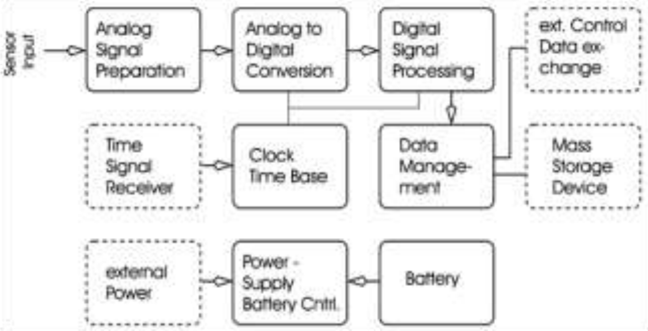

Figure 1: Typical components of a Data recorder, dashed boxes are optional [7]

Our approach was the creation of a data recorder that consists of four main subsystems, described in the figure 2. Its difference from the typical approach of a data recorder is that the triggering process, the time stamping and further analysis that needs to be performed, is not accomplished inside the data recorder. It is implemented on the next module of the system, which is called main board and is equipped with a GPS receiver for time-stamping and geo-location services, a powerful quad-core processor and a communication protocol that can alert civilians and public services using IEEE 802.15.4 protocol.

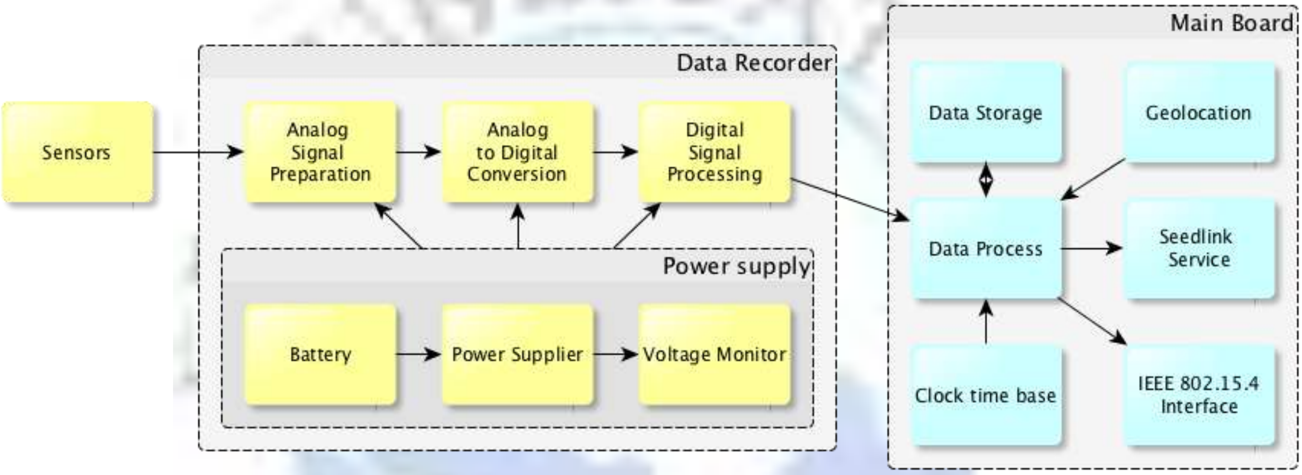

Figure 2: The designed approach

- Analog Signal Preparation: incoming signals from the sensors are amplified and filtered.
- Analog to Digital Conversion: after the filtering process signals are digitized using a 24-bit Analog to Digital Converter (ADC).
- Digital Signal Processing: data are transformed into counts and are transferred into packets to the main board so they can be analyzed and time-stamped.
- Power supply and voltage monitoring: A custom voltage monitor is responsible for the protection of the system from over and under-voltage. By suppressing voltage fluctuations faults can be avoided [8]

Sensors

Our recorder is capable of accepting a tri-axial accelerometer and a tri-axial geophone as inputs for seismic signals. It is compatible with sensors that are commonly used in commercial seismic recorders. By default, it is equipped with an LIS344ALH accelerometer and a three axis LGT-4.5 geophone. It has been proved by experimental data that low cost Micro ElectroMechanical Systems (MEMS) sensors can be used in seismic research, and their measurements are comparable with the measurements of the relevant electromechanical sensors [9].

Geophone

Our geophone sensor has a resonant frequency of 4.5Hz. Despite the fact that 4.5Hz geophones are not preferred for recording earthquake activity they are capable of recordings down to 0.3Hz without any special filtering [10]. Thus, our sensor is capable of recording the seismic signals that are important for seismic data analysis. In table 1 a brief description of the LGT-4.5 sensor follows. The manufacturer provided all parameters except for the spring constant that had to be calculated from equation (1). Furthermore the geophone sensors, one for each axis, are sealed on an IP-67 rated enclosure that includes a leveling tool so that the sensors can be aligned perfectly.

$$f_{res} = \frac{1}{2\pi} \cdot \sqrt{\frac{K}{m}} \tag{1}$$

Table 1: LGT-4.5 specifications

Parameter	Symbol	Value	Tolerance (%)	Units
Resonant Frequency	f_o	4,5	±10	Hz
Coil Mass	m	0,0113	-	Kg
Damper Constant	D	0,707	±10	N/(m/s)
Spring Constant	K	9,0336	±10	n/m
Generator Constant	G	28,8	±10	V/(m/s)
Coil resistance	R_{coil}	375	±5	Ω

As soon as a motion is detected from the sensor, the mass of the geophone moves along the direction of its axis. The motion of the mass can be described by equation (2), where the relative position of the mass X_r for the applied acceleration $\ddot{X}_h$ on the sensor is described as a function in the frequency domain

$$V_i = \frac{X_r}{\ddot{X}_h} = \frac{-1}{s^2 + \frac{D}{m}s + \frac{K}{m}} \tag{2}$$

During the motion of the mass along the axis of motion, interaction takes place between the mass and the magnetic field generated by a permanent magnet that is attached within the sensor. According to Faraday's Law expressed in the frequency domain (3), and due to the fact that $\partial\Phi/\partial t$ is considered constant for small displacements, the output voltage is proportional to the coil's velocity.

$$V_o = \frac{\partial\Phi}{\partial t} = \frac{\partial\Phi}{\partial t}\frac{\partial x}{\partial t} = -Gs\dot{X}_r = -GsX_r \tag{3}$$

Derived from (2,3), the transfer function of the sensor for a given acceleration and velocity input is shown in the following equations (4,5). A plot of their frequency response is shown in figure 3.

$$H_{acc}(s) = \frac{V_o}{V_i} = \frac{GsX_r}{\frac{X_r}{\ddot{X}_h}} = \frac{Gs}{s^2 + \frac{D}{m}s + \frac{K}{m}} = \frac{28.8s}{s^2 + \frac{0.707}{0.0113}s + \frac{9.0336}{0.0113}} = \frac{28.8s}{s^2 + 62.56s + 799.4} \; (4) \tag{4}$$

$$H_{vel}(s) = \frac{V_o}{V_i} = \frac{GsX_r}{\frac{X_r}{\dot{X}_h}} = \frac{Gs^2}{s^2 + \frac{D}{m}s + \frac{K}{m}} = \frac{28.8s^2}{s^2 + \frac{0.707}{0.0113}s + \frac{9.0336}{0.0113}} = \frac{28.8s^2}{s^2 + 62.56s + 799.4} \; (5) \tag{5}$$

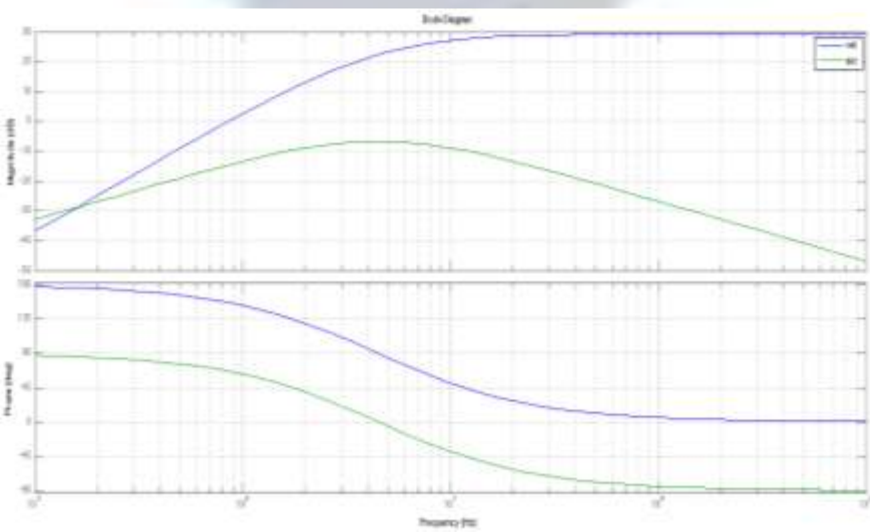

Figure 3: Frequency response plot for velocity (blue) and acceleration (green) of LGT-4.5

Accelerometer

MEMS sensors have mainly digital output and can be interfaced via SPI or I_2C protocols. The internal analog to digital converters (ADC) that are embedded on the digital accelerometers renders them inappropriate for our system, because of the low resolution of the ADC's. Our accelerometer has an analog output and selective range of ±2g and ±6g and has a very low noise margin of $50\mu g/\sqrt{Hz}$ per axis. By using previous experimental data by Müller [11], showed in figure 4a, the sensitivity of each axis is illustrated. From that data we estimated the transfer function of each axis, x, y, z (6,7,8) respectively and their plots are illustrated in figure 4b.

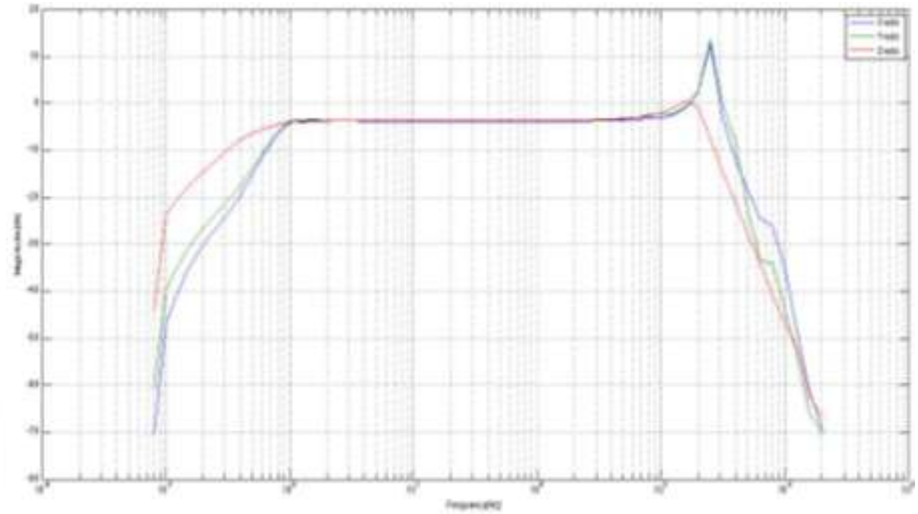

4a

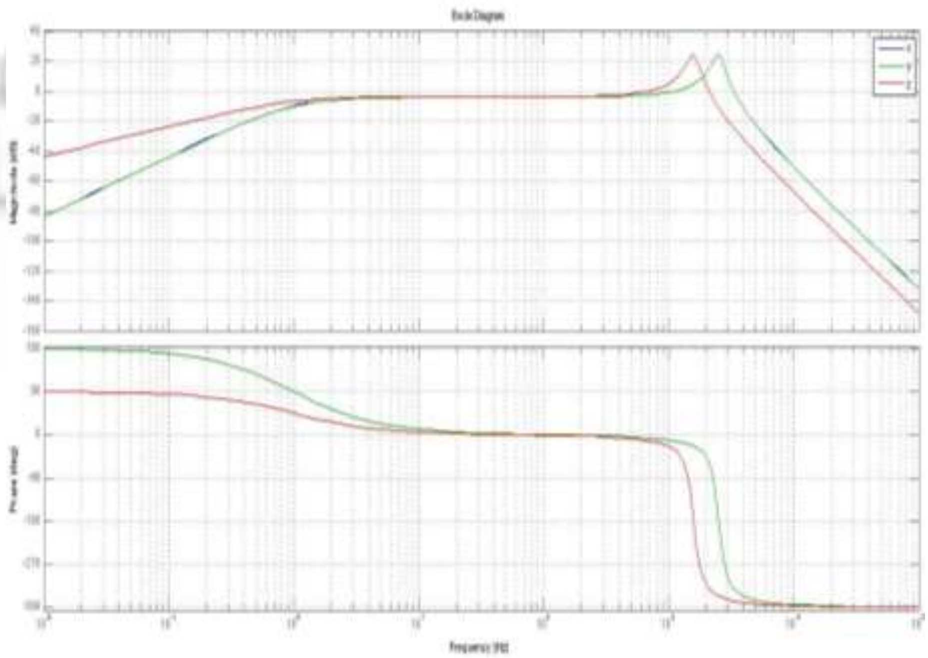

4b

Figure 4a: Magnitude plot of the measurements, 4b Magnitude and phase plot from the estimated transfer functions (blue: x-axis, green: y-axis, red: z-axis)

$$G_x(s) = \frac{4.048e16s^2}{s^6 + 6346s^5 + 5.114e08s^4 + 1.593e12s^3 + 6.28e16s^2 + 7.89e17s + 2.47e18} \quad (6)$$

$$G_y(s) = \frac{4.006e16s^2}{s^6 + 6346s^5 + 5.114e08s^4 + 1.593e12s^3 + 6.28e16s^2 + 7.89e17s + 2.47e18} \quad (7)$$

$$G_z(s) = \frac{6.493e15s}{s^5 + 3996s^4 + 2.03e08s^3 + 3.982e11s^2 + 9.896e15s + 6.215e16} \quad (8)$$

The accelerometer board has also an internal RC low-pass filter, by selecting the appropriate capacitor value; the cut-off frequency can be altered. We have placed a 3nF capacitor, so the cut-off frequency of the filter is now f_c= 482.28 Hz.

Analog Signal Preparation

Analog signal preparation (A.S.P.) module is responsible for receiving the input signals from the sensors and preparing them for digitization on the next module of the system. The total process requires two steps; amplification and filtering. Firstly, the amplification takes place using a high gain (64db) differential input amplifier, and secondly the filtering is achieved using a fourth order Butterworth filter with cut-off frequency fc= 500Hz. Both the amplifier and the filter use ultra low noise operator amplifiers with a noise margin of about $3\mathrm{nV}/\sqrt{\mathrm{Hz}}$. In equation (9) the transfer function of both the amplifier and the filter is expressed, while in figure 5 the frequency response plot is illustrated.

$$G(s) = \frac{1.623e17}{s^4 + 8209s^3 + 3.37e07s^2 + 8.102e10s + 9.741e13} \tag{9}$$

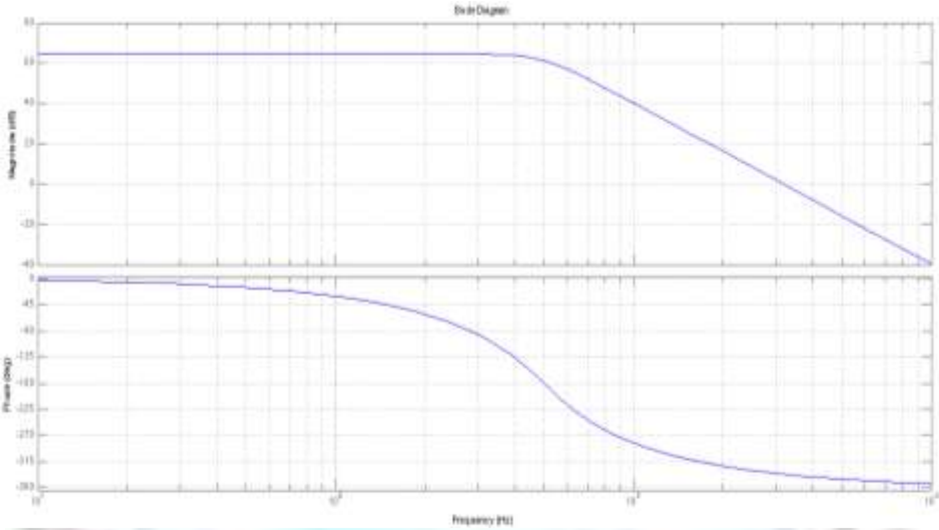

Figure 5: Frequency response of A.S.P.

Analog to Digital Conversion

Once the signals are amplified and filtered, they are driven to the next module of the recorder where they are digitized. Our digitizing module is an ADS1256EVM analog to digital converter that operates at 7.68MHz, capable of receiving up to eight analog inputs. Three are used for the accelerometer's inputs and three are used for the seismometer's inputs. Finally the last two inputs are used for voltage and temperature readings. This ADC is capable of converting data with 24-bit resolution. It communicates via SPI protocol for communicating with the CPU. After its initialization it is configured to cycle among the channels and converting the analog data into digital. The sample rate has been selected to 100 samples per sec, keeping in mind that the sampling process should be performed according to this rule:$f_s \geq 2f_n$. The equation (10) presents the frequency response of the 5th-order low pass sinc filter that is embedded in the ADC. Our module can be configured with many parameters, such as the appropriate sample rate, the programmable gain amplifier with values from one to sixty-four, and de/activating the internal buffer. Alteration of these values lead to changes in the effective number of bits (ENOB). According to our configuration and by solving (11) the effective number of bits in our configuration is set to 23.4 bits.

$$|H(f)| = |H_{sinc^5}(f)| \cdot |H_{averanger}(f)| = \left| \frac{\sin\left(\frac{256\pi \cdot f}{f_{clkin}}\right)}{64 \cdot \sin\left(\frac{4\pi \cdot f}{f_{clkin}}\right)} \right|^5 \cdot \left| \frac{\sin\left(\frac{256\pi \cdot Num_{Ave} \cdot f}{f_{clkin}}\right)}{Num_{Ave} \cdot \sin\left(\frac{256\pi \cdot f}{f_{clkin}}\right)} \right| \tag{10}$$

$$ENOB = \frac{\ln\left(\frac{Full\_scale\_range}{RMS_{noise}}\right)}{\ln 2} \tag{11}$$

Digital Signal Processing

Responsible for the communication with the digitizing module and the mainboard as well is a Stellaris Launchpad board, equipped with a Cortex – M4 CPU operating at 80MHz. After the SPI interface has been initialized, the Launchpad writes to the ADS1256 registers commands, in order to configure the behavior of the digitizing module. The configuration of the digitizing module is rather extensive; it includes options such as selecting the appropriate gain, buffer, data rate, or even the endianness of the data. After a new configuration has been written on the ADS1256 registers the device has to be idle for a specific settling time. By issuing the appropriate commands the CPU forces the ADC to cycle its inputs and convert them into numbers formatted as complement of two. The readings are stored into a packet as signed integers with each value ranging from–8388608 to 8388607 counts. A flow-chart of the firmware's basic operations is illustrated in figure 6; as it can be seen it is rather large, so only few important functions are displayed. Also in table 2 a packet consisting of digitized data from the eight channels of the recorder is described. Except formatting the data into packets, it is crucial that our device operates correctly at temperatures between -40 to 80C°. For that reason it is equipped with a temperature sensor that can be applied inside the recorders boxing and can measure the ambient temperature of the system. A custom supplier connected with a battery provides the necessary voltages that are needed for the normal operation of the recorder. If the battery's voltage drops below a given threshold, the recorder will start to malfunction, and if the voltage is at a critical low level, it will probably cause permanent damage to the battery. For the afore mentioned reasons, the voltage of the battery is measured, digitized and observed by the recorder.

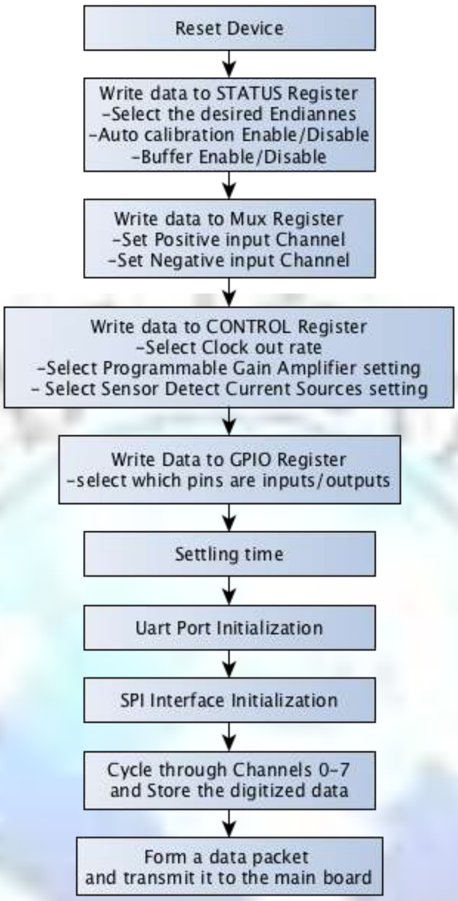

Figure 6: Basic operation of the firmware

Table 2: Description of the transmitted packet

Description of Data	X_acc	Y_acc	Z_acc	X_geo	Y_geo	Z_geo	Volt	Temp
Size of data (bytes)	4	4	4	4	4	4	4	4

Our data recorder is not equipped with a timing signal receiver, nor does it execute any triggering algorithms. These tasks are performed in the main board, were a GPS receiver synchronizes the system time. Furthermore, digitized data from the recorder are parsed, transformed into velocity and acceleration data and also further processing via triggering algorithms is performed. Finally, the data is formed into mini-seed in order to be transmitted on a seed link server for storage purposes and to be displayed on a web user interface (UI).

Voltage monitoring – Fault tolerance

As mentioned above our implementation, operates with a custom power supplier that is connected to a battery. Voltage monitoring is crucial in embedded systems, because due to over/under-voltage, hardware failure may occur (Permanent Faults). Experimental data showed that when integrated circuits are exposed to voltage fluctuations they tend to produce more errors than during their operation with stable voltage [12]. Based on the above data, a monitoring circuit that alerts and protects the recorder for sudden voltage fluctuations has been designed so that permanent and transient errors can be suppressed. Furthermore, by adding proper EMI shielding on cables and enclosure, intermittent faults can also be suppressed. Finally in case EMI noise has been added to the digitized data it can be canceled by the digital filter that is implemented on the ADC. Finally, the integrity of the sensors can be verified by the activation of an option on the control register of the ADS1256 that will notify the system when a channel malfunctions.

Conclusion/Results

In this article we have discussed the design of a low cost earthquake recorder, which can be utilized either for education and research purposes, or even commercial use. We have fully analyzed the mathematical models of both the sensors and the ASP that are related to this system. Furthermore, we have suggested a method of error reduction that will aid the uninterrupted operation of our recorder. Finally, by using an interface circuit our recorder is capable of bearing commercial sensors. Further studies on this project would involve the addition of an ADC module with resolution greater than 24 bits, the implementation of an ASP with selective gain and even lower noise, and the upgrade of the firmware code.

Acknowledgment

The first author wishes to express his gratitude to the Kalliniki Dendrinou - Antonakaki Institution for the fellowship that has been provided.

References

[1]. Yih-Min Wu, Hiroo Kanamori, “Development of an Earthquake Early Warning System Using Real-Time Strong Motion Signals”, Sensors2008, vol. 8,issue 1, pp. 1-9.

[2]. Yutaka Nakamura, Jun Saita “FREQL and AcCo for a Quick Response to Earthquakes”,“Earthquake Early Warning Systems”, Springer 2007, p. 308.

[3]. Richard M. Allen, “The ElarmS Earthquake Early Warning Methodology and Application across California”, Earthquake Early Warning Systems”, Springer 2007, pp. 21-44.

[4]. Richard M. Allen, “Earthquakes, early and strong motion warning ”,Encyclopedia of Solid Earth Geophysics, Springer 2011, pp. 1-13.

[5]. H. Serdar Kuyuk, Richard M. Allen, “Optimal Seismic Network Density for Earthquake Early Warning: A Case Study from California”, Seismological Research Letters Volume 84, Number 6, November-December 2013, pp. 1-9.

[6]. IRIS Instrumentation Committee,”Global Seismographic Network Data Logger Specifications”, 2003, pp. 1-10.

[7]. Asch, G.: “Seismic Recording Systems”, New Manual of Seismological Observatory Practice (NMSOP), Deutsches GeoForschungsZentrum GFZ 2009, p. 2.

[8]. S. Voutsinas, G. Dilintas,"Necessity of supervision circuits on embedded systems", International Scientific Conference eRA-8 - Production Control Session, 2013, pp. 1-6.

[9]. Elizabeth S. Cochran, Jesse F. Lawrence, Anna Kaiser, Bill Fry, Angela Chung, Carl Christensen ,Comparison between low-cost and traditional MEMS accelerometers: a case study from the M7.1 Darfield, New Zealand, aftershock deployment , ANNALS OF GEOPHYSICS, vol 54, issue 6, 2011, pp. 728-737.

[10]. J. Havskov, Gerardo Alguacil, Instrumentation in Earthquake Seismology ,Springer, 2010, p. 68.

[11]. Swen Müller , Ronaldo da Silva Dias, Ingrid Driele da Silva Santos, “MEMS ACCELEROMETER PERFORMANCE”, ICSV18,2011, p. 7.

[12]. Narayanan V. ,Yuan Xie, “Reliability concerns in embedded system designs”, IEEE Computer Society Computer Volume:39, Issue: 1, 2006.